Journal of the Argentine Chemical Society

EFFECT OF ACID OXIDATION TREATMENT ON ADSORPTION PROPERTIES OF ARC-DISCHARGE SYNTHESIZED MULTIWALL CARBON NANOTUBES

José L. Vicente[1], Alberto Albesa[1], Jorge L. Llanos[1], Ethel S. Flores[1], Abel E. Fertitta[1], Delia B. Soria[2], M. Sergio Moreno[3] and Matías Rafti[1,♥]

[1]Instituto de Investigaciones Fisicoquímicas Teóricas y Aplicadas (INIFTA), Dpto. de Química, Fac. de Cs. Exactas, Universidad Nacional de La Plata. Diag 113 y 64 (1900) L.P., Prov. Bs. As., Argentina.

[2]Centro de Química Inorgánica (CEQUINOR), Dto. de Química, Fac. Cs. Exactas, Universidad Nacional de La Plata. 47 y 115, CC. 962 (1900) L.P. , Bs. As., Argentina.

[3]Centro Atómico Bariloche (CAB), San Carlos de Bariloche, (8400) Río Negro, Argentina.

Received April 4, 2011. In final form August 31, 2011.

Abstract

The effect of nitric/sulfuric acid oxidation treatment on commercial arc-discharge multiwall carbon nanotubes was studied. Purification and structure modifications were assessed via Transmission Electron Microscopy and Thermogravimetric Analysis; while changes in adsorption properties were monitored by nitrogen and methane adsorption isotherms. After treatment, nitrogen isotherms

♥ Corresponding author. Email: mrafti@quimica.unlp.edu.ar

present hysteresis loop and an increased BET surface area; while adsorption energies obtained from isosteric heat profiles revealed a marked decrease. We propose an explanation for these findings and use macroscopic experimental data to gain insight on acid oxidation effect on the material.

Keywords: multiwall carbon nanotubes; methane adsorption; acid oxidation

Resumen

Se estudió el efecto de la oxidación ácida por medio de mezclas sulfúrico/nítrico, de nanotubos comerciales de pared múltiple sintetizados por el método de la descarga de arco. Para evaluar el grado de pureza y las modificaciones estructurales se utilizaron las técnicas de Microscopía Electrónica de Transmisión y Termogravimetría; mientras que los cambios en las propiedades de adsorción fueron monitoreados por medio de la realización de isotermas a distintas temperaturas utilizando gases simples como Nitrógeno y Metano. Luego del tratamiento oxidativo, se observó la aparición de ciclos de histéresis en las isotermas al mismo tiempo que el área superficial según BET se incrementó. Por otro lado, los calores isostéricos obtenidos evidenciaron una disminución importante. Proponemos una explicación posible para estos hallazgos y hacemos uso de la información experimental obtenida para revelar detalles del mecanismo de oxidación de los Nanotubos.

Palabras clave: nanotubos de carbón de pared múltiple; adsorción de metano; oxidación ácida

Introduction

While Single wall Carbon Nanotubes (SWCNT) were first reported by Ijima in 1991 [1], Multi Wall Carbon Nanotubes (MWCNT) were discovered a few decades before by Radushkevich et al. (see reference [2] for a detailed discussion). Due to their unique mechanical, electrical and chemical properties carbon nanotubes (CNT) have prompted a wide variety of potential applications [3,4,5,6]), among them, the use in storage systems for alternative fuels (e.g.; natural gas) [7]. Single-walled carbon nanotubes (SWCNT) consists of a single graphite layer wrapped into a cylindrical tube, while Multi-walled carbon nanotubes (MWCNT) are formed by a number of such structures concentrically nested. The most common methods for CNT synthesis are catalyst-enhanced chemical vapor deposition (CVD), arc-discharge, and laser ablation [8]. As produced CNT samples usually contain a considerable amount of impurities depending on the synthesis method used (e.g.; amorphous carbon, metal catalyst); and are generally close-ended with a fullerene-like cap [9]. Due to availability and costs reasons, methods for purification, functionalization and opening of MWCNT constitute a research area of great interest. In particular, it is well known that acid oxidation (HNO_3/H_2SO_4 mixtures) leads to remarkable structural changes, and there has been in the past several efforts oriented to elucidate the extent of these modifications under different conditions [10,11,12,13]. Strong acid oxidative conditions were used in the present study to treat MWCNT samples. The effect on purity, structure, and (having in mind potential use on storage systems for alternative fuels) adsorption properties were studied through different physical methods. Structural characterization was conducted via Transmission Electron Microscopy (TEM) and Thermogravimetric Analysis (TGA). Adsorption isotherms using nitrogen (N_2) and methane (CH_4) were conducted. BET surface areas and isosteric heats of adsorption were calculated.

Experimental

General

All the reagents used for oxidation treatment were of analytical grade. MWCNT produced by arc-discharge process were purchased from NanoCraft Inc (about 30-40% purity, with nano-onion like and nano-polygonal particles, with 5-20 nm diameter and 300-2000 nm long). A two-step acid oxidation treatment as described by Li et al. [11] was applied to the MWCNT sample; and it

can be summarized as follows,

• 4 hour bath-sonication in 500 ml 6 M HNO_3. Dilution with distilled water in order to quench the oxidation reaction and cool down to ambient temperature. Filtration in a 0.22 μm Millipore polycarbonate membrane, rinsing with distilled water up to neutral pH, and overnight vacuum drying.

• 4 hour, 120ºC reflux in concentrated $H2SO_4/HNO_3$ (3:1) mixture; followed by filtration and drying as described above.

This procedure is a pre-treatment process because it can only remove the unreacted catalyst (when MWCNT were produced via CVD synthesis), [11]. As-produced MWCNT used in this work do not contain such impurities (see sec. 3.2 for TGA experimental confirmation), but for the sake of comparison with previous results, the complete two-step procedure was applied. Efficiency of the whole operation is ≈ 15 − 20% mass-loss.

Materials and Equipment

Adsorption isotherms were measured volumetrically employing Pyrex conventional equipment. Pressures were determined using absolute capacitance manometers, KS−Baratron 122AA − 00010AB, with 1.0×10^{-3} Torr maximum error. Temperature was thermostatically controlled and measured with a digital thermometer, Altronix equipped with Pt − 100(DIN) sensor head, previously calibrated against an oxygen vapor pressure thermometer with 0.1 ºC precision. Matheson Gas Products were used in all the experiments, with more than 99% purity. Isosteric heat of adsorption (Qst) can be calculated from two isotherms determined at close but different temperatures, T_1 and T_2, via the following expression,

$$Qst = \frac{RT^2}{T_1 - T_2} \ln \frac{p_2}{p_1},$$

where p_1 and p_2 are the equilibrium pressures at temperatures T_1 and T_2, when the amount of adsorbed gas is constant, and T is the corresponding mean temperature. TGA was performed with Shimadzu T GA − 50 unit, at 5ºC/min heating rate, and 50 ml/min oxygen flow. All TEM images presented in this work were acquired using a Philips CM200 UT microscope operated at 200 kV and room temperature.

Results and Discussion

Transmission Electron Microscopy

As-produced (NanoCraft Inc.) MWCNT material consists in, mostly close-ended, nanotubes together with some amount of nano-onion like and graphite impurities typical of arc-discharge synthesis process. Onion-like carbon particles are also known to appear when CNT are subjected to severe nitric acid oxidation treatment [14]. TEM images of the as-produced sample are shown in Figure 1; a closer inspection reveals the CNT dimensions to be roughly, 5 − 20 nm diameter and 100 − 2000 nm long; while a great majority shows capped ends. In figure 2, TEM images of treated sample can be observed. A careful comparison with the as-produced MWCNT reveals the appearance of further amorphous carbon layers on the nanotube walls, and partial opening of the originally closed ends.

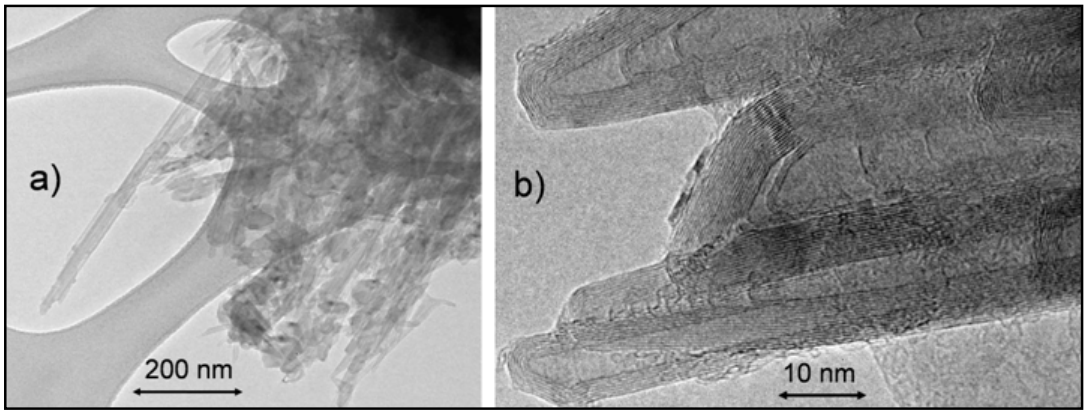

Figure 1. a) TEM image of the as-produced MWCNT sample, where a variety of nanotube lengths can be observed, together with some amount of impurities. b) Magnified image showing MWCNT closed ends, and typical size of inner cavities.

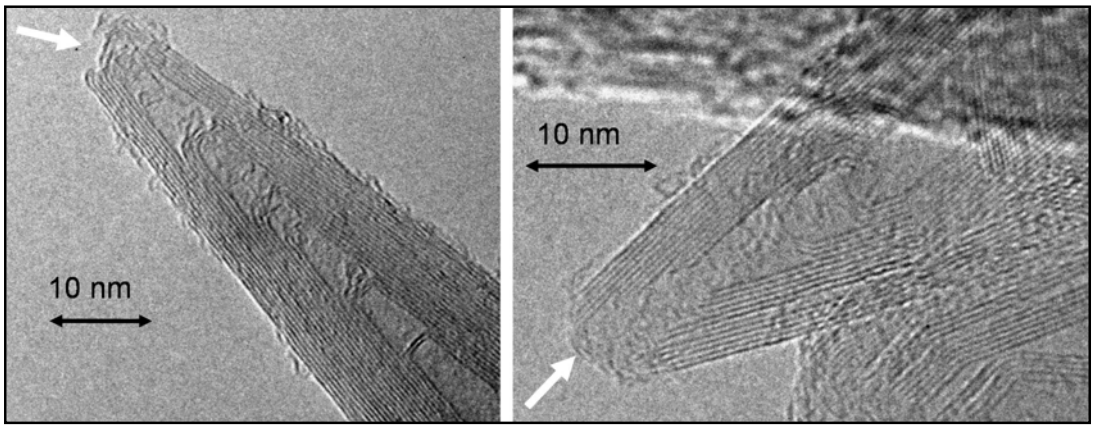

Figure 2. TEM images of the acid oxidized MWCNT sample, where some examples of the uncapping achieved can be observed (white arrows used as indications).

Thermogravimetric Analysis

Thermogravimetric Analysis (TGA) technique has been extensively used for CNT characterization [15,16,17]. In principle, the mass-loss temperature profile obtained in a typical experiment depends on a number of factors; among them, the preparation method (e.g.; if metal-catalyst residues from CVD synthesized CNT are present, TGA will depend on its concentration and identity), and proportion of carbonaceous material other than CNT present on the sample (e.g.; amorphous or graphitic carbon). McKee and Vecchio, [16] observed the following trends when comparing TGA profiles for CVD synthesized MWCNT, amorphous carbon, and graphitic carbon samples. High-purity graphite mass loss start was observed at approx. 630ºC, with maximum oxidation rate at 850ºC (the presence of transition metals was found to decrease temperature for oxidation); while MWCNT showed a lower temperature peak burn of rate at approx. 600ºC.

Amorphous carbon presents the highest reactivity with maximum oxidation rate at approximate 500ºC. However, when considering arc-discharge synthesized MWCNT instead of CVD, the high temperatures and electric fields applied (together with the lack of metal-catalyst residue), cause a lower defect density, and consequently, an increased stability towards oxidation processes. Figure 3 displays TGA profile obtained for the sample before acid oxidation; it can be observed the lack of mass-loss below 600ºC which indicates absence of amorphous carbon. Maximum oxidation rate temperature was determined to be 785ºC with ash content of < 0.6% above 900ºC. In the other hand, TGA experiments conducted after oxidative treatment show distinctive features, as can be observed in Figure 4. While previously discussed high-temperature behavior remains unchanged; for temperature ranges between 200 − 600ºC mass loss is ≈ 20%. This fact is a strong indicator of the appearance of surface defects and/or amorphous carbon as a consequence of acid treatment.

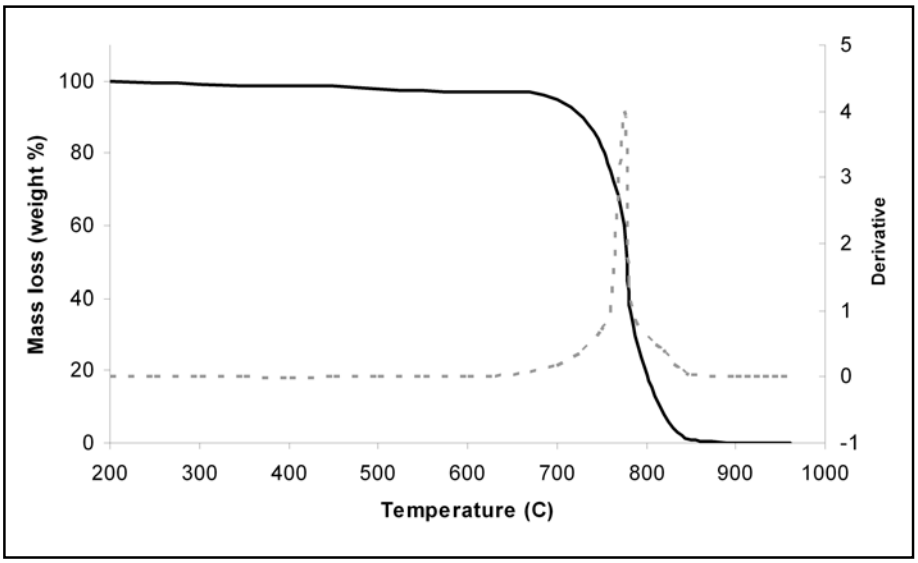

Figure 3. Mass loss curve (full line) and derivative (broken line) obtained from TGA experiments for the as-produced MWCNT sample. The lack of material loss for T<600ºC ranges, and the absence of residue when T>950ºC indicates that both amorphous carbon, and metal catalyst residue contamination, respectively, can be ruled out.

Also, the creation of functional groups affects the properties of the material [18]. Graphs were normalized in every case using the sample weight at 150ºC (at this temperature only water and adsorbed organic impurities are removed from the surface with no carbon oxidation whatsoever).

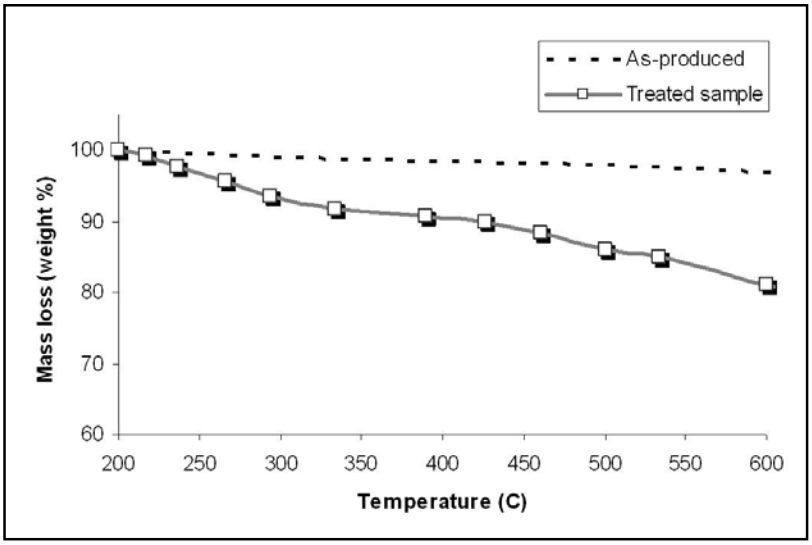

Figure 4: Comparison between TGA of as-produced and treated MWCNT sample. For the acid oxidized sample, an earlier mass-loss start is observed, which indicates presence of amorphous carbon.

N_2 isotherms and BET area

Nitrogen adsorption isotherms were measured for MWCNT samples subjected to acid oxidation treatment as described above; results can be observed in Figure 5. BrunauerEmmet-Teller (BET) theory was used in order to monitor changes in surface area, while pore size distribution was obtained applying Barret-Joyner-Halenda equation [19,20]. Two ranges of different behavior can be observed in Figure 5 as relative pressure (p/p0) increases. For low pressures ($0 < p/p0 < 0.4$) adsorbed volume increases slowly, indicating monolayer completion. The absence of a steep increase at very low p/p0 reflects the absence of micropores with sizes in the order of magnitude of the nitrogen molecule. For pressures corresponding to ($0.4 < p/p0 < 1.0$), hysteresis loop can be observed, which can be related to capillary condensation on mesopores. According to IUPAC classification categories, isotherms can be labeled as Type II or Type IV depending on the existence of hysteresis or not in the adsorption-desorption loop (see ref. [21]). Capillarity is known to occur in small mesopores of 2 − 4 nm size, precisely the order of magnitude of the inner cavities of MWCNT as shown in TEM images (see above).

Therefore, the origin of the hysteresis loop can be traced back to a partial uncapping of the MWCNT as a result of acid oxidation. The steep increase near p/p0 =1.0 accounts for the presence of larger pores on the surface; aggregates of CNT were found to cause such effect in previous studies [20].

Kuznetzova et al. [22] argued, for the case of SWCNT, that acid oxidation provokes the appearance of functional groups on the surface (e.g; CO, COOH), that cause a diminished adsorption capacity, and slower kinetics for the process. However, for MWCNT a different tendency was found; table 1 reflects a significant increase in BET surface area and total pore volume after acid oxidation. These findings are in line with recently published work by Liu et al., for ozone oxidation pre-treatment [6]. Estimative calculations of BET surface area increment to be expected when achieving a complete CNT uncapping indicate a much higher value than reported in table 1. Nevertheless, the surface area increment observed, together with hysteresis loop on adsorption-desorption isotherm, allows speculating on a partial uncapping of the as-produced sample.

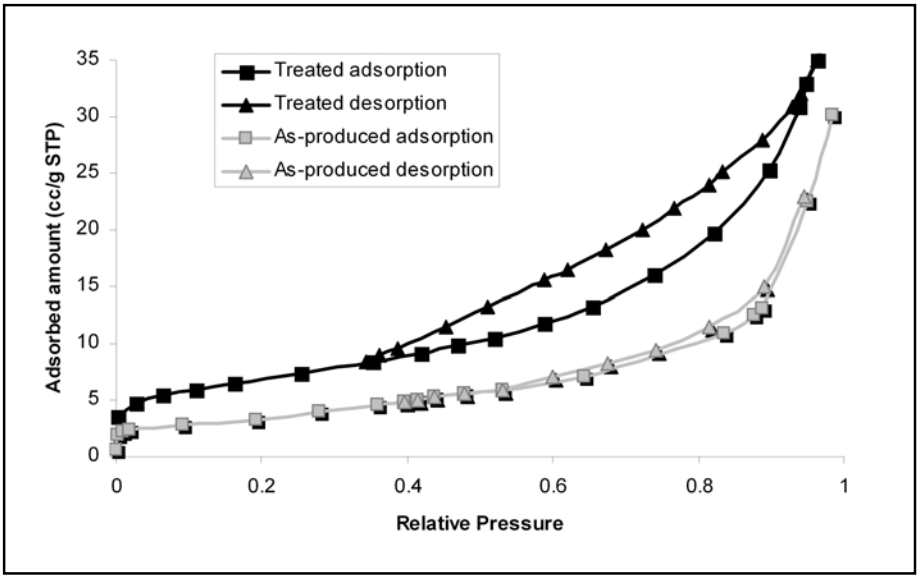

Figure 5: Nitrogen adsorption-desorption isotherm of as-produced and treated MWCNT samples, showing two different behavior regarding hysteresis. Temperature was fixed at −196.15ºC. The error bars are indicated by the size of the symbols used for representing the data points. This applies also to all other figures unless the error bars are explicitly given.

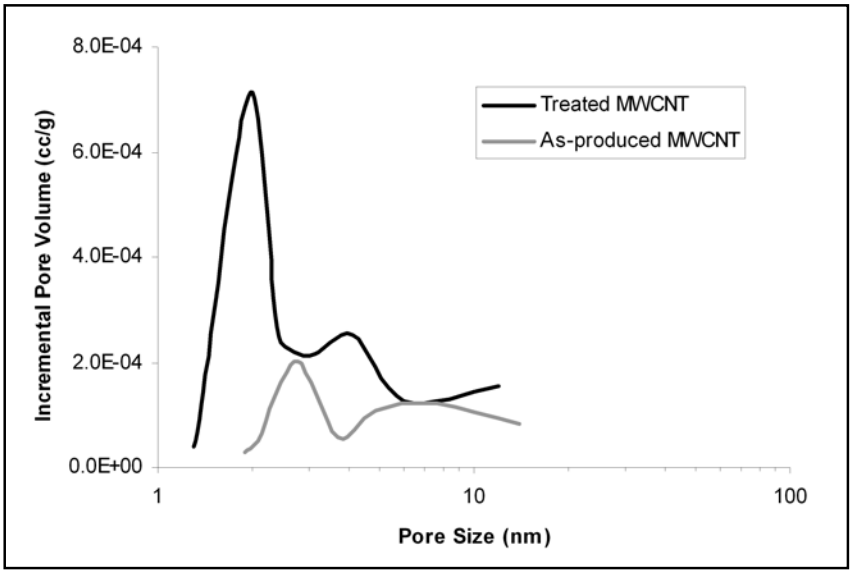

Figure 6: Pore size distribution for treated and as-produced MWCNT sample. A reduction of the peak height in incremental pore volume and a shift to lower values can be observed after wet oxidation (shift peak from ≈ 3.0 nm to 2.0 nm with a small shoulder in both cases.

Table 1: BET surface area and total pore volume for treated and as-produced MWCNT samples.

M\CNT sample	BET Surface Area m_2/g	Total Pore Volume cc/g
As-produced	12.1	0.038
Treated	26.8	0.059

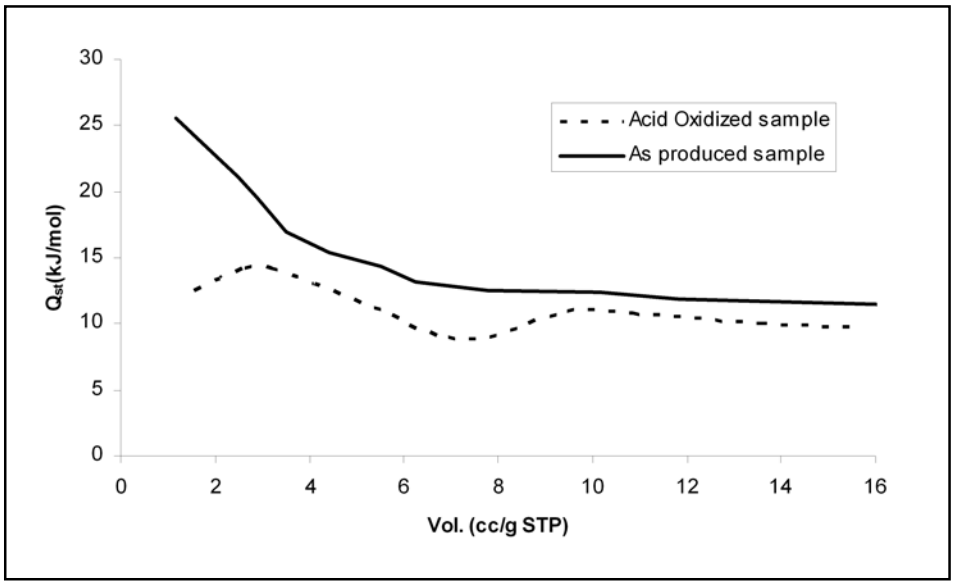

Figure 7: Isosteric heat of adsorption profle for methane on treated and as-produced MWCNT sample as determined for $T_1 = -170$ºC and $T_2 = -180$ºC. A remarkable decrease can be observed after acid oxidation.

CH_4 isosteric Heat of Adsorption

The ability to adsorb methane is an important parameter when assessing suitability for use in alternative fuels storage systems of a given adsorbent material. Having the latter in mind, methane adsorption isotherms were measured for MWCNT samples at different temperatures, and using eq. 1, isosteric heat of adsorption (Qst) profiles were calculated. Figure 7 shows results obtained, which are in line with recent published experimental and simulations data for similar systems [23]. Considering structural differences discussed in sec. 3.3, a much higher heat of adsorption would be expected for the treated sample due to contribution of more energetic sites inside CNT. However, profiles in Figure 7 reveal a dramatic decrease in Qst when comparing as-produced and treated samples; moreover, after acid oxidation greatly resembles the behavior founded for methane on graphite surfaces [23]. This apparent contradiction can be rationalized by assuming that; either the

inner space of MWCNT is not accessible for methane molecules or, there is not a significant amount of such uncapped structures (the first argument can be ruled out by simple comparison of CH_4 and N_2 cross-sectional areas). Diminished energy for adsorption sites after treatment reveals that surface has suffered modification up to some extent. It can be speculated that, high energy groove sites on CNT bundles (as experimentally detected by Weber et al. [24]), are no longer exposed due to the blockage of amorphous carbon generated with acid oxidation. This fact would explain both surface area increase, and modification of adsorption energy profile.

Conclusions and Outlook

The consequences of acid oxidation treatment applied can be summarized as follows; i) multi-stage nitrogen adsorption isotherm featuring hysteresis loop, ii) increase of BET surface area, iii) decrease of isosteric heat of adsorption for methane, iv) appearance of amorphous carbon (as evidenced via TEM images and TGA profiles), and v) partial uncapping of originally closed MWCNT. Acid oxidation causes a decrease of adsorption energies; it can be assumed that new sites were created either via removal of carbon atoms at the highly strained fullerene cap of MWCNT ends, or at wall-defects with equally lower activation energies. This hypothesis is supported by the finding of an increased adsorption capacity after treatment. One possible explanation of the above mentioned features is that, groove sites on initially present CNT bundles were lost due to blockage by amorphous carbon deposited during acid oxidation. This would explain both increase of surface area and decrease in the adsorption energy profile [25,12]. In order to gain further insight regarding effect of surface modification of CNT on adsorption properties, Monte Carlo simulations for nitrogen and double walled carbon nanotubes are being carried, the final goal is to be able to make meaningful comparisons with experimental results. In this work, conventional surface analysis methods were used in order to diagnose the extent of damage provoked. "Au contraire" than previous published results, stronger oxidation conditions are required if the goal is to achieve total uncapping of MWCNT. Moreover, if the material was produced via arch-discharge synthesis, acid treatment can be safely applied in order to eliminate inherent carbonaceous impurities on the sample without risk of undesired extensive damage to the CNT structure. Further effort will be directed towards characterization of the combined effect of stronger acid oxidation with complementary procedures such as air oxidation on structure and properties of MWCNT.

Acknowledgments. The authors gratefully acknowledge financial support from the UNLP (Universidad Nacional de La Plata), CICPBA (Comisión de Investigaciones Científicas de la Prov. de Buenos Aires, Argentina) and CONICET (Consejo de Investigaciones Científicas y Tecnológicas-Argentina).

References

[1] S. Ijima. *Nature*, **1991**, *354*, 6348.

[2] M. Monthioux and V.L. Kuznetsov. *Carbon*, **2006**, *44*, 1621-1623.

[3] R.H. Baughman, A.A. Zakhidov, and W.A. de Herr. *Science*, **2002**, *297*, 787-792.

[4] S. Crossley, J. Faria, M. Shen, and D.E. Resasco. *Science*, **2009**, *327*, 68-72.

[5] W.J. Guan, Y. Li, Y.Q. Chen, X.B. Zhang, and G.Q. Hu. *Biosensors and Bioelectronics*, **2005**, *21*, 508-512.

[6] Z.Q. Liu, J. Ma, Y.H. Cui, and B.P. Zang. *Appl. Catal. B*, **2009**, *92*, 301-306.

[7] D. Lozano-Castello, J. Alcaniz-Monge, M.A. de la Casa-Lillo, D. Carzola-Amoros, and A. Linares-Solano. *Fuel*, **2002**, *81*, 1777-1803.

[8] R.G. Ding, G.Q. Lu, Z.F. Yan, and M.A. Wilson. *Journal of Nanoscience and Nanotechnology*, **2001**, *1(23),* 7-29.

[9] P.J.F. Harris. *Critical Reviews in Solid State and Materials Sciences*, **2009**, *30*, 235-253.

[10] R. Marega, G. Accorsi, M. Meneghetti, A. Parisini, M. Prato, and D. Bonifazi. *Carbon*, **2009**, *47(3)*, 675-682.

[11] Y. Li, X. Zhang, J. Luo, W. Huang, J. Cheng, Z. Luo, T. Li, F. Liu, G. Xu, X. Ke, L. Li, and H.J. Geise. *Nanotech*., **2004**, *15*, 1645-1649.

[12] Y.S. Park,Y.C. Choi, K.S. Kim, D-.C. Chung, D.J. Bae, K.H. An, S.C. Lim, X.Y. Zhu, and Y.H. Lee. *Carbon*, **2001**, *39*, 655-661.

[13] M.T. Martinez, M.A. Calleias, A.M. Benito, M. Cochet, T. Seeger, A. Anson, J. Schreiber, C. Gordon, C. Marhic, O. Chauvet, J.L.G. Fierro, and W.K. Maser. *Carbon*, **2003**, *41*, 2247-2256.

[14] C. Bower, A. Kleinhammes, Y. Wu, and O. Zhou. *Chem. Phys. Lett.*, **1998**, *288*, 481-486.

[15] F. Lu, X. Wang, M.J. Meziani, L. Cao, L. Tian, M.A. Bloodgood, J. Robinson, and Y.P. Sun. *Langmuir*, **2010**, *26(10)*, 7561-7564.

[16] G.S.B. McKee and K.S. Vecchio. *J. Phys. Chem. B*, **2006**, *110*, 1179-1186.

[17] D. Bom, R. Andrews, D. Jacques, J. Anthony, B. Chen, M.S. Meier, and J.P. Selegue. *Nanoletters*, **2002**, *2(6)*, 615-619.

[18] A.B. Gonzalez-Guerrero, E. Mendoza, E. Pellicer, F. Alsina, C. Fernandez-Sanchez, and L.M. Lechuga. *Chem. Phys. Lett.*, **2008**, *462*, 256-259.

[19] E.P. Barret, L.G. Joyner, and P.P. Halenda. *J. Am. Chem. Soc.*, **1951**, *73*, 373-380.

[20] Q.H. Yang, P.X. Hou, S. Bai, M.Z. Wang, and H.M. Cheng. *Chem. Phys. Lett.,* **2001**, *345*, 18-24.

[21] F. Li, Y. Wang, D. Wang, and F. Wei. *Carbon*, **2004**, *42*, 2375-2383.

[22] A. Kuznetsova, D.B. Mawhinney, V. Naumenko, J.T. Yates JR, J. Liu, and R.E. Smalley. *Chem. Phys. Lett.*, **2000**, *321*, 292-296.

[23] A.G. Albesa, J.L. Llanos, and J.L. Vicente. *Langmuir*, **2008**, *24*, 3836-3840.

[24] S.E. Weber, S. Talapatra, C. Journet, A. Zambano, and A.D. Migone. *Phys. Rev. B*, **2000**, *61(9)*, 13150-13155.

[25] A. Bougrine, N. Dupont-Pavlovsky, A. Naii, J. Ghanbaia, J.F. Mareche, and D. Billaud. *Carbon*, **2001**, *39*, 685-695.